

STUDY OF THE POWER DEPOSITION IN THE LHC LOW-BETA INNER TRIPLET FOR A Nb3Sn DESIGN

G. Ambrosio, F. Broggi, INFN - LASA, Via F.lli Cervi 201, 20090 Segrate (Mi), ITALY

Abstract

In this paper the power deposited in the Nb3Sn coils of the inner quadrupole triplet of the LHC low-beta insertions (for a second generation design) is studied as a function of the gradient and of the aperture.

Starting from the reference "Yellow Book" case, different configurations are investigated in order to get the best working conditions, using the higher performance of the Nb3Sn with respect to the NbTi.

The temperature increase in the coils is then evaluated by ANSYS simulations to check the stability margin of the magnets.

1 INTRODUCTION

The better superconducting magnetic performances of Nb3Sn respect to NbTi allow to design insertions with higher focusing gradient or with larger aperture with the same gradient[1],[2]. This would allow higher machine performances either in the collision optics or in the beam dynamics.

The main case studied is for a quadrupole aperture of 70 mm, with a gradient of 235 T/m and 30 mm diameter collimator, without absorbers (reference case). The comparison with higher gradient (300 T/m) in the same aperture and of larger aperture (85 mm) with the same gradient is done. The effect of stainless steel absorbers 5 mm thick under the quadrupoles in the reference case is discussed together with the effect of absorbers of different thickness under each quad (suited absorber case).

2 ASSUMPTIONS

- The studied part of the insertion[3] extends from the interaction point (I.P.) to the last quadrupole of the inner triplet and is composed by four magnets (Q1,Q2a,Q2b,Q3) 5.5 m long with aperture of 70 mm starting at 23 m from the I.P. A trim quadrupole (Q01) 1.5 m long with aperture of 85 mm is between Q1 and Q2a at 30 cm from Q1. Before Q1 (at 19 m from I.P.) a 1.8 m long copper collimator, with aperture of 30 mm (28 in one of the case treated) is placed.

The magnetic field is assumed as purely hard edge quadrupole field with the DFFD sequence for the secondary particles (D=defocusing, F=focusing). The gradient of Q01 is 82 T/m when the main quad gradient is 235 T/m and is scaled as the main gradient varies.

In addition a finite solenoid simulating a detector is considered; its maximum field is 2 T, radius 1.1 m, 5.3 m long centered at I.P. The beam pipe aperture before the

collimator is 63 mm, after the collimator it is 63 or 78 mm for quad aperture of 70 or 85 mm respectively. The thickness of the absorbers, when considered, is 5 mm under all the quadrupoles for the uniform absorber case; in the suited absorber case the thickness is 12 mm under Q1, 10 mm under Q01, 4.5 mm under Q2a, Q2b and Q3.

- 7+7 TeV p-p events are generated by the DTUJET code[4], the crossing angle of the two beams at the I.P. is 200 μ rad, the nominal luminosity 10^{34} cm⁻²s⁻¹ and a total cross section of 80 mbarn is considered. The secondary particles realised are tracked in the magnetic structure of the low β insertion with our analytical code. As the particles hit the stainless steel beam pipe, 1.5 mm thick, they are processed by FLUKA code[5].

- In FLUKA the quadrupole geometry is defined as precisely as possible both in its geometrical shape and in its material composition. The cut-off values are 1 MeV for the hadrons, 1.5 MeV for the electrons and positrons, 0.2 MeV for the photons and 0.4 eV for the neutrons.

The power deposition in the magnet is stored both as integral, region by region as in the geometry definition, i.e. for each shell (or layer), each insulation between the shells, each pole wedge, aluminium collar and iron yoke, and in binning volumes in order to obtain the local power distribution and localise the maximum peak power. For the 70 mm aperture the binning geometries used have a squared section of about 24.3 mm² and 5.86 mm² with a length of 50 cm (parallel to the axis of the beam). The latter section is used with a longitudinal length of the bins of 10 cm too. For 85 mm aperture the bin sections are 25 mm² and 6.25 mm², while the length is always 50 mm.

3 POWER DEPOSED

For all the cases, except the suited absorbers one, the hottest quadrupole is Q2a; in the case with the suited absorbers, the hottest quadrupole is the last one with a total power deposited of 14.6 W, much less than the power deposited in Q2a in the other cases. In tab.1 the power deposited in the quads is shown together with the peak power density in Q2a for the different binning volumes (in cm³) considered. The cases are identified by two numbers indicating the aperture and the gradient of the main quad when a third number is indicated it refers to the trim quad gradient (i.e. 70-235(-82) means: aperture 70 mm, main gradient 235 T/m, trim quad gradient 82 T/m). The symbol * indicates the case with uniform absorbers, while † refers to the suited absorber case. The maximum peak power occurs in the first half meter of the Q2a, on the

horizontal plane. For the different binning the statistical error, as from different runs with independent random seeds, is 3%, 4% and 5% respectively. In Fig. 1 the maximum peak power density is plotted as a function of the longitudinal coordinate for all the cases considered.

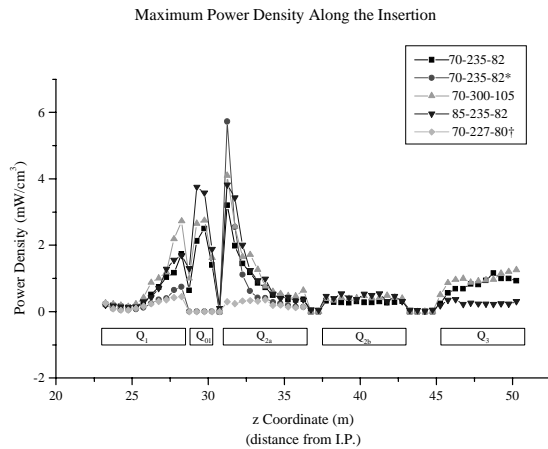


Figure 1: Maximum power density along the insertion. The dimensions of the bins are $0.493 \times 0.493 \times 50 \text{ cm}^3$ for quad aperture of 70 mm, and $0.5 \times 0.5 \times 50 \text{ cm}^3$ for 85 mm quad aperture. See text for the legend explanation.

In Fig. 2 the maximum peak power density in the second quadrupole obtained with the small binning volume is shown. The case of the smallest binning for the reference case is shown too (open square).

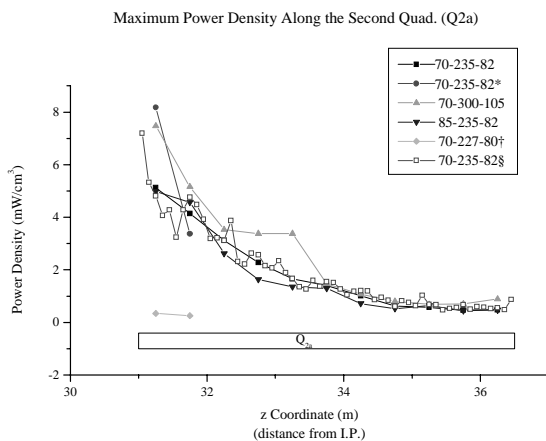


Figure 2: Maximum power density in Q2a. The dimensions of the bins are $0.242 \times 0.242 \times 50 \text{ cm}^3$ for quad aperture of 70 mm, and $0.25 \times 0.25 \times 50 \text{ cm}^3$ for 85 mm quad aperture. In the case § the bin length is 10 cm. See text for the legend explanation.

As we can see from Fig. 2 the maximum power deposition is in the first part of the quadrupole.

The values obtained with 10 cm length of the bins are distributed around the values got with 50 cm, so the mean

behaviour is well fitted by the binning with such dimensions and it is useless to use smaller binning.

In Fig 3 the azimuthal power distribution is shown at radius of 3.63 cm, for aperture of 70 mm, and radius of 4.4 cm for aperture of 85 mm, i.e. where the maximum peak power in the shell is realised.

As in Fig 2 the smallest binning is plotted with open square (§).

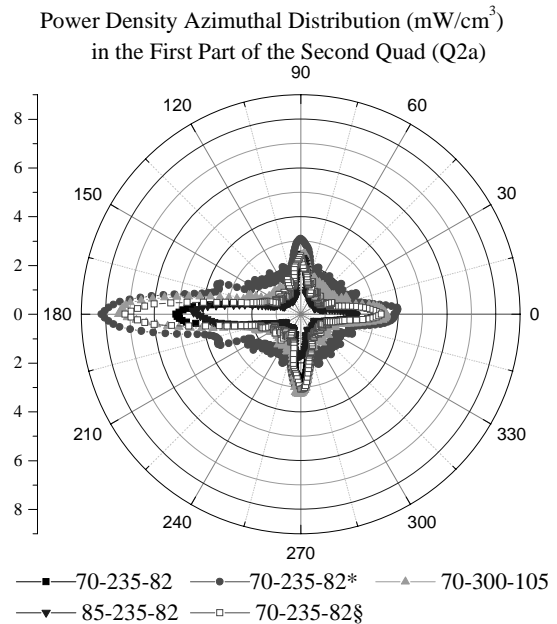


Figure 3: Azimuthal power density distribution at radius of 3.63 cm (aperture 70 mm) and 4.4 cm (aperture 85 mm) for binning volume as in Fig.2. The case of suited absorber is not shown, being the power much lower.

The data obtained show that the use of absorbers not always is efficient because it can lead to an increase of the power deposited, like in the case of uniform cylindrical absorbers, both in the total power and in the peak power.

This because the smaller aperture of the absorbers does start the cascade of particles that would travel longer depositing their energy elsewhere in the last quadrupoles where there are not critical conditions. So the use of the absorbers must be carefully evaluated and their dimensions suited for the particular case.

Moreover the case with higher gradient is more critical respect to the reference case, being higher both the total power deposited in the quads and the peak power. The 85 mm aperture seems more safety regarding the total power, but the peak power is about the same than in the reference case. The thermal analysis gives the operating conditions and safety margins for the various cases.

4 THERMAL ANALYSIS

The power deposition data were input in a 2-D FE model for a steady state, linear thermal analysis with the

ANSYS code. In the collars the total deposited power was concentrated in few mesh elements near the mid-plane, in the other regions the FLUKA local power distribution has been used. We have evaluated analytically that heat conduction in the magnet length is few percent: so a 2-D model, considering the peak power instead of the average one, is a good, slightly conservative, approximation.

pole wedge is made of bronze. Heat exchange to helium (1.9 K) occurs through the surface of the inner bore and through the outer surface of the collars. For the heat transfer coefficient a conservative value of 1000 W/m²K has been used. In tab.1 the peak temperatures in the coils, in the inner layer (mid-plane), in the cable where is the peak field and the maximum heat flux toward helium are shown for both types of collars. The peak temperature is

Tab.1 Summary of the data; only the volume of the bins for $\Phi=70$ mm is reported, see text for 85 mm. On the second line is the power in the absorbers. * = cylindrical absorbers †= suited absorbers

Case	Total power (W)					Peak Power in Q2a (mW/cm ³)			Thermal Behaviour				
	Q1	Q01	Q2a	Q2b	Q3	Volume (cm ³)			Collar material	max. Temp. (K)			peak flux W/m ²
						12.2	2.9	0.6		Coil	layer1	peak B	
70-235	11.5	8.7	22.4	7.5	17.4	3.2	5.1	7.2	s.steel	2.6	2.45	2.24	46
									Al	2.33	2.33	2.11	31
70-235*	12.1	6.5	27.5	10.3	14.5	5.7	8.2	9.8	--	--	--	--	--
Abs.	5.6	5.0	11.0	8.5	11.0								
70-300	14.4	11.0	25.3	9.5	20.4	4.1	7.5	--	s.steel	2.74	2.6	2.3	56
									Al	2.45	2.45	2.15	41
85-235	10.6	8.2	19.4	8.0	6.3	3.8	5.0	--	s.steel	2.43	2.34	2.12	33
									Al	2.25	2.25	2.05	26
70-227†	13.3	4.5	10.8	7.8	14.6	--	0.3	0.7	--	--	--	--	--
Abs.	12.2	4.3	4.9	5.3	10.6								

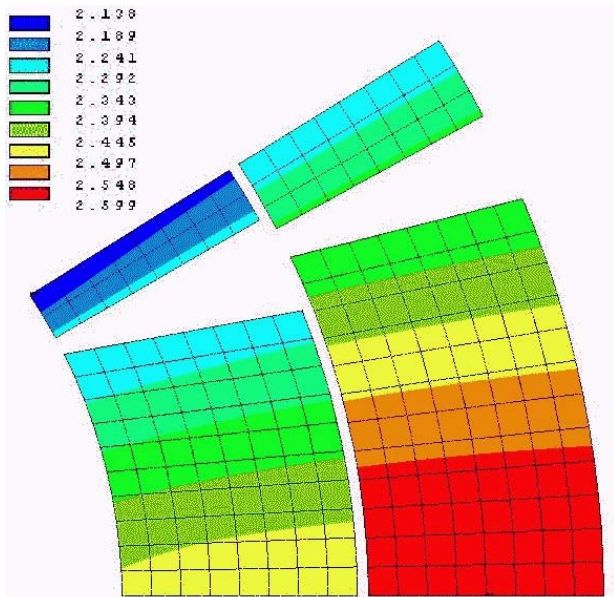


Figure 4: Temperature distribution in the two layers for the case 70-235-82. The collar is of stainless steel.

The quadrupole cross section was described in details.

The thermal conductivity of each layer has been computed with a simple conservative model representing the layer as a pile of alternating cables and insulation (G10). In the cables the heat is supposed to flow only through the pure copper of each strand (i.e. no thermal conduction between adjacent strands is considered). The collars are made of stainless steel or aluminium alloy. The

on the mid-plane, in the first or second layer according to the collar material, while the lower transition temperature is located where the peak field occurs (i.e. near the pole). A map of the temperature in the coil cross section is shown in Fig. 4 for the 70-235-82 design with s.steel collars.

5 CONCLUSIONS

This detailed analysis confirms the conclusions already stated in ref.[6] where a 0.5 K temperature increment was supposed, showing that the power deposition by the radiation is acceptable without endangering the low-beta quad operation also at superfluid helium temperature.

Nb3Sn is a good solution for the second generation of the low beta inner triplet quadrupole, either for increasing the gradient or the quadrupole aperture.

REFERENCES

- [1] G.Ambrosio et al. "Preliminary proposal ...", I.N.F.N Report. I.N.F.N./TC - 95/25, 13/Sep/1995.
- [2] S.Caspi et al. "Design of a Nb3Sn High Gradient ...", Proc. of MT-15, Beijing (10/97).
- [3] "LHC Conceptual Design", Tech. Rep., CERN, October 1995, CERN/AC/95-05.
- [4] P.Aurenche et al. "DTUJET-93", Computer Physics Comm., vol 83, pp. 107,1994.
- [5] A. Fassò et al. "FLUKA: Present status and ...", IV Int.Conf. On Calorimetry in HEP, p.493,1994.
- [6] G.Ambrosio et al. "Stability of a Nb3Sn low-beta quadrupole ...", EPAC96, Sitges, pp.2293.